J. Fluid Mech. (1975), *vol.* 69, *part* 4, *pp.* 673–688
Printed in Great Britain

Ergodic properties of inviscid truncated models of two-dimensional incompressible flows

By C. BASDEVANT AND R. SADOURNY
Laboratoire de Météorologie Dynamique du C.N.R.S., Paris, France

(Received 4 January 1974)

The equilibrium spectra of two-dimensional numerical model flows are studied from the viewpoint of microcanonical ensemble averages. The method leads to accurate numerical verification of the ergodic, or mixing, hypothesis in the case of systems constrained to a finite number of degrees of freedom.

1. Introduction

It is well known that turbulence theory is somewhat outside the scope of classical statistical mechanics, primarily because it involves systems with an infinite number of degrees of freedom in the limit of vanishing viscosity. Nevertheless, this tool can in fact be successful in providing some insight into the dynamic processes of turbulence (Onsager 1949; Kraichnan 1967). For instance, the statistical properties of inviscid model flows constrained to a finite number of degrees of freedom can be thoroughly investigated by means of statistical mechanics. The knowledge we are able to gain in this manner is of primary interest to anyone involved in numerical simulation of the Navier–Stokes equations. Apart from a better understanding of the model's behaviour, it provides an explanation for the discrepancy between the dynamics of numerical models and real-fluid dynamics, described by observations or by theories of turbulence.

The typical approach of classical statistical mechanics is to explain the statistical behaviour of a system in terms of its structural properties, the most common of these being energy conservation. A similar standpoint has been recognized in the recent trends of turbulence theory, as emphasized by the use of stochastic models, such as the test-field model (Kraichnan 1971*a*) or the MRCM model (Frisch, Lesieur & Brissaud 1974).

Now, the dynamics of three-dimensional flow appear to be essentially governed by the existence of a single quadratic invariant: the total kinetic energy of the flow. This property should thus be built into any numerical (truncated) model of the flow, in order to preserve the structure of nonlinear interactions. It may then be shown by statistical mechanics, and well verified in actual simulations, that an inviscid finite system evolves towards an equipartition of energy among all Fourier modes (Orszag 1970). However, the situation is quite different for real flows, which evolve towards the well-known $k^{-\frac{5}{3}}$ (Kolmogorov) energy spectrum, characterized by an energy cascade towards higher wavenumbers. We thus see a significant alteration in the statistical properties of the system, due only to the

existence of a truncation. It is clear that the infinite number of degrees of freedom in the three-dimensional Navier–Stokes equations is a most important structural property, which must however be violated by numerical simulation.

The situation is quite different in two dimensions since the dynamics of the flow are then governed by the simultaneous conservation of two invariant quadratic forms: the total enstrophy and the total energy of the flow. Following the same considerations as before, both properties should be built into the numerical model, in order to get the proper structure of nonlinear interactions. In this case, significant discrepancies between the statistical properties of real flows and their truncated models have been emphasized by Kraichnan (*1971b*) and investigated numerically by Fox & Orszag (1973), Deem & Zabusky (1971) and Lilly (1969). This means that in two dimensions, as well as in three, the truncation brings about a fundamental alteration in the structure of the problem.

Our purpose here is to derive analytical expressions for the equilibrium spectra in the inviscid truncated case, from the viewpoint of microcanonical ensemble averages. Various numerical experiments will show actual convergence of time averages towards the theoretical expressions.

2. Definition of the truncated fluid-dynamic problem

A two-dimensional non-divergent flow is entirely described by a single scalar function of space and time (the stream function), which we denote by $\psi(\mathbf{x}, t)$. In the inviscid case, the governing equation reads

$$\partial(\Delta\psi)/\partial t + J(\psi, \Delta\psi) = 0, \tag{1}$$

where the symbol J refers to the Jacobian operator.

In the case of a pure initial-value problem with twofold periodicity of the stream function, this equation can be written in spectral form using the Fourier series $\hat{\psi}(\mathbf{k}, t)$. In the truncated problem, the Fourier series is replaced by a finite sum restricted to N vector modes belonging to a finite array D, and the generic form of the governing equation reads

$$\frac{d}{dt}\hat{\psi}(\mathbf{k}, t) + \sum_{\substack{\mathbf{p}+\mathbf{q}=\mathbf{k} \\ \mathbf{k},\,\mathbf{p},\,\mathbf{q}\in D}} \frac{P^2}{K^2}\, a(\mathbf{p}, \mathbf{q})\, \hat{\psi}(\mathbf{p}, t)\, \hat{\psi}(\mathbf{q}, t) = 0. \tag{2}$$

In this equation, $a(\mathbf{p}, \mathbf{q})$ is a function depending on the choice of the truncated Jacobian J_*: $a(\mathbf{p}, \mathbf{q}) = \mathbf{p} \wedge \mathbf{q}$ if J_* is computed in spectral form. P and K are 'pseudo-wavenumbers' related to eigenvalues $-P^2$ and $-K^2$ of the truncated Laplacian Δ_*, corresponding to eigenfunctions $e^{-i\mathbf{p}.\mathbf{x}}$ and $e^{-i\mathbf{k}.\mathbf{x}}$: $P = |\mathbf{p}|$ and $K = |\mathbf{k}|$ if Δ_* is computed in spectral form.

We shall restrict our attention to inviscid truncated models conserving exactly the enstrophy as well as the energy of the flow, in order to get the correct structure for nonlinear interactions. In fact, this is equivalent to imposing for any given wave-vector triad $(\mathbf{k}_1, \mathbf{k}_2, \mathbf{k}_3)$ with $\mathbf{k}_1 + \mathbf{k}_2 + \mathbf{k}_3 = 0$

$$\Sigma\, K_i^2\, a(\mathbf{k}_i, \mathbf{k}_j) = \Sigma\, K_i^2\, K_l^2\, a(\mathbf{k}_i, \mathbf{k}_j) = 0,$$

where the summations are taken over all permutations (i, j, l) of $(1, 2, 3)$. These

properties are straightforward in the case of direct truncation in Fourier space. They may also be verified when J_* is a finite-difference Jacobian belonging to the class initially derived by Arakawa (1966).

3. The ergodic hypothesis

If the truncated system is defined by N real time-dependent variables, the construction of the corresponding phase space is well known. The set of wave vectors is split into three parts:

$$D = D_1 + D_2 + D_3,$$

where D_1 is the subset corresponding to real values of $\hat{\psi}$ and D_2 and D_3 are two subsets chosen in such a way that, for any $\mathbf{k}_2 \in D_2$, there is a $\mathbf{k}_3 \in D_3$ such that $\hat{\psi}(\mathbf{k}_3, t)$ is the complex conjugate of $\hat{\psi}(\mathbf{k}_2, t)$. The co-ordinates in phase space are chosen as follows:

$$y(\mathbf{k},t) = \begin{cases} 2^{-\frac{1}{2}} K \hat{\psi}(\mathbf{k},t) & \text{if} \quad \mathbf{k} \in D_1, \\ K \operatorname{Re} \hat{\psi}(\mathbf{k},t) & \text{if} \quad \mathbf{k} \in D_2, \\ K \operatorname{Im} \hat{\psi}(\mathbf{k},t) & \text{if} \quad \mathbf{k} \in D_3. \end{cases}$$

It has been shown (cf. Orszag 1970) that the motion in this phase space is non-divergent. This can be seen at once from the generic form of (2), since for any proper Jacobian, whether truncated or not,

$$a(\mathbf{p},\mathbf{q}) = 0 \quad \text{when} \quad \mathbf{p} = 0 \quad \text{or} \quad \mathbf{q} = 0,$$

which implies that $d\hat{\psi}(\mathbf{k},t)/dt$ is independent of $\hat{\psi}(\mathbf{k},t)$. This in turn implies, obviously, that $dy(\mathbf{k},t)/dt$ is independent of $y(\mathbf{k},t)$, so that

$$\frac{\partial}{\partial y(\mathbf{k},t)} \left(\frac{d}{dt} y(\mathbf{k},t) \right) = 0.$$

We can then apply Liouville's theorem, asserting that the natural motion in phase space conserves the measure of any measurable set of states.

Starting from any initial state with energy E and enstrophy Z, the trajectory of $M(t)$ stays on the $(N-2)$-dimensional intersection S of the hypersphere

$$\sum_{\mathbf{k} \in D} y^2(\mathbf{k},t) = E \tag{3}$$

with the hyperellipsoid

$$\sum_{\mathbf{k} \in D} K^2 y^2(\mathbf{k},t) = Z. \tag{4}$$

When S is considered together with the measure induced by the Lebesgue measure in the phase space, (2) defines a stochastic process on S. Since the problem is a pure initial-value problem, a consequence of Liouville's theorem is that this stochastic process is stationary. We shall be interested only in the ergodic properties of the phase function $y^2(\mathbf{k})$. Composition of this phase function with the stochastic process on S defines a stationary stochastic process $y^2(\mathbf{k},t)$ with time averages

$$U(\mathbf{k},T) = \frac{1}{T} \int_0^T y^2(\mathbf{k},t)\, dt.$$

The random function $U(\mathbf{k}, T)$ is the average energy in mode $\mathbf{k}$ within a portion of the trajectory. The process $y^2(\mathbf{k}, t)$ will be ergodic if $U(\mathbf{k}, T)$ converges towards the expectation of $y^2(\mathbf{k})$ as $T \to \infty$. If we look for convergence in the quadratic mean, we may write, denoting expectations by square brackets and defining $U(\mathbf{k}) = [y^2(\mathbf{k})]$,

$$[(U(\mathbf{k}, T) - U(\mathbf{k}))^2] = \frac{1}{T^2} \int_0^T \int_0^T R_{\mathbf{k}}(t, t')\, dt\, dt',$$

where $R_{\mathbf{k}}(t, t')$ is the time covariance:

$$R_{\mathbf{k}}(t, t') = [(y^2(\mathbf{k}, t) - [y^2(\mathbf{k}, t)])\,(y^2(\mathbf{k}, t') - [y^2(\mathbf{k}, t')])].$$

Hence, convergence of $U(\mathbf{k}, T)$ towards $U(\mathbf{k})$ in the quadratic mean is equivalent to

$$\frac{1}{T^2} \int_0^T \int_0^T R_{\mathbf{k}}(t, t')\, dt\, dt' \to 0 \quad \text{as} \quad T \to \infty, \tag{5}$$

which means that two successive states of the system become uncorrelated as the time lag becomes large enough. Further, the first theorem of Birkhoff (see for instance Khinchin 1949, p. 19) states that there is an almost sure limit for $U(\mathbf{k}, T)$ on S, since the process is stationary. Then the 'mixing' hypothesis (5) implies convergence of the time average to the expectation $U(\mathbf{k})$ not only in the quadratic mean, but even almost everywhere on S.

We intend now to give experimental support for the mixing hypothesis first by computing the expectations $U(\mathbf{k})$ in phase space, and then by computing the time average of numerical solutions of (2).

4. Computation of the expected energy spectrum

In order to simplify the problem, we first notice that $\mathbf{k}$ does not appear explicitly, except as an index or through the function K. Hence $U(\mathbf{k})$ is in fact a function $U(K)$ only. We can define the order of multiplicity of a 'mode' K as the number of original vector modes $\mathbf{k}$ which correspond to this particular value of K. We shall sort all distinct values of K and refer to them from now on as $K_1 < K_2 < \ldots < K_n$. We have of course

$$N = \sum_{i=1}^{n} \alpha_i,$$

where α_i is the order of multiplicity of K_i. Accordingly, $U(K_i)$ is conveniently denoted by U_i. Further, we shall call $\bar{K}$ the average 'pseudo-wavenumber' K with respect to the energy distribution, in short $\bar{K}^2 = Z/E$ [see (3) and (4)]. The analytical expression for the expected energy spectrum is straightforward, using the measure induced on S by the Lebesgue measure. Taking into account the internal symmetries of the problem, the expression for U_i reads

$$U_i = \frac{1}{\alpha_i} \frac{\int_V Y_i \left(\prod_{j=1}^{n} Y_j^{\beta_j} \right) dY_3 \ldots dY_n}{\int_V \left(\prod_{j=1}^{n} Y_j^{\beta_j} \right) dY_3 \ldots dY_n}, \tag{6}$$

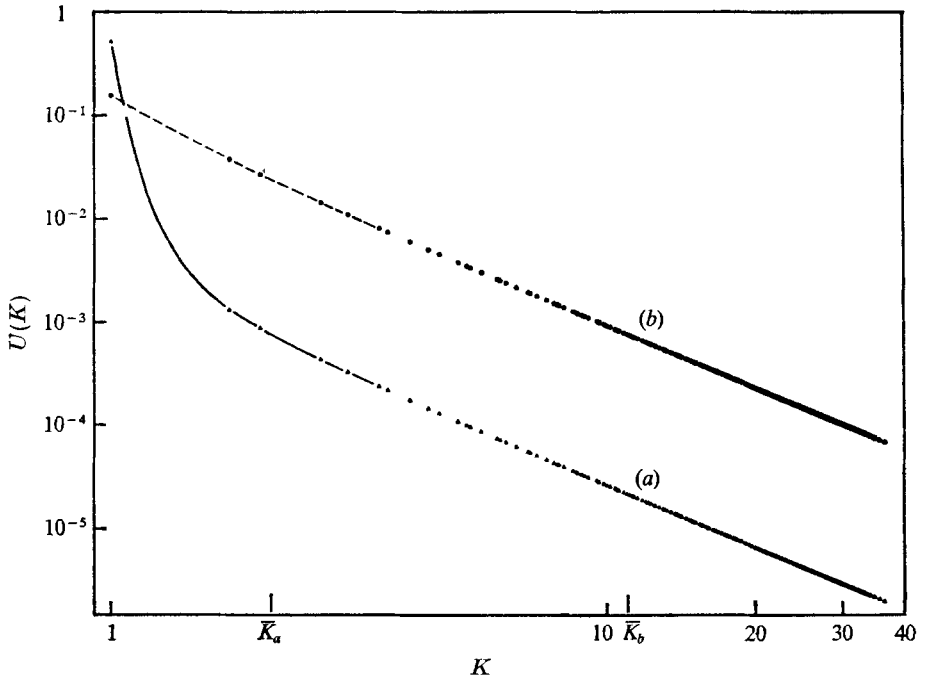

FIGURE 1. Theoretical spectra for a 64×64 grid; $E = 3{\cdot}141$ (log–log scale). (*a*) $\bar{K} = 2{\cdot}1$. (*b*) $\bar{K} = 11$.

where $\beta_j = \frac{1}{2}\alpha_j - 1$ and V is defined by

$$\left.\begin{gathered} \sum_{j=1}^{n} Y_j = E, \quad \sum_{j=1}^{n} K_j^2 Y_j = \bar{K}^2 E, \\ Y_j > 0 \quad (j > 2) \end{gathered}\right\} \tag{7}$$

together with $Y_1, Y_2 > 0$.

Although (6) is an exact analytical form, it leads to exceedingly long calculations owing to the large number of variables involved. In the slightly restrictive case where β_2 is even, one can derive upper and lower bounds for U_i, which lead to accurate approximations in several important cases. These bounds are given in appendix A for the case $\beta_1 = \beta_2 = 2$, which corresponds to the numerical experiments. The estimate (A 4) is extremely accurate when $\bar{K}$ is close to either K_1 or K_n, for instance in the cases shown in figure 1. It is not as good if $\bar{K}$ is near the middle of the interval $[K_1, K_n]$. Of course, we are primarily interested in the asymptotic behaviour of the spectrum as $n \to \infty$. The reader is invited to refer to appendix B for the corresponding derivations. We just state the main results here.

For a pseudo-wavenumber distribution $K_1, K_2, \ldots, K_n$ with orders of multiplicity $\alpha_1, \alpha_2, \ldots, \alpha_n$, the expected energy spectrum of a system possessing N degrees of freedom, a given energy E and a given enstrophy $\bar{K}^2 E$ is asymptotically equivalent to

$$U(K_1) = \frac{E}{\alpha_1}, \quad U(K_i) = \frac{E}{N} \frac{\bar{K}^2 - K_1^2}{K_i^2 - K_1^2} \quad (i > 1), \tag{8}$$

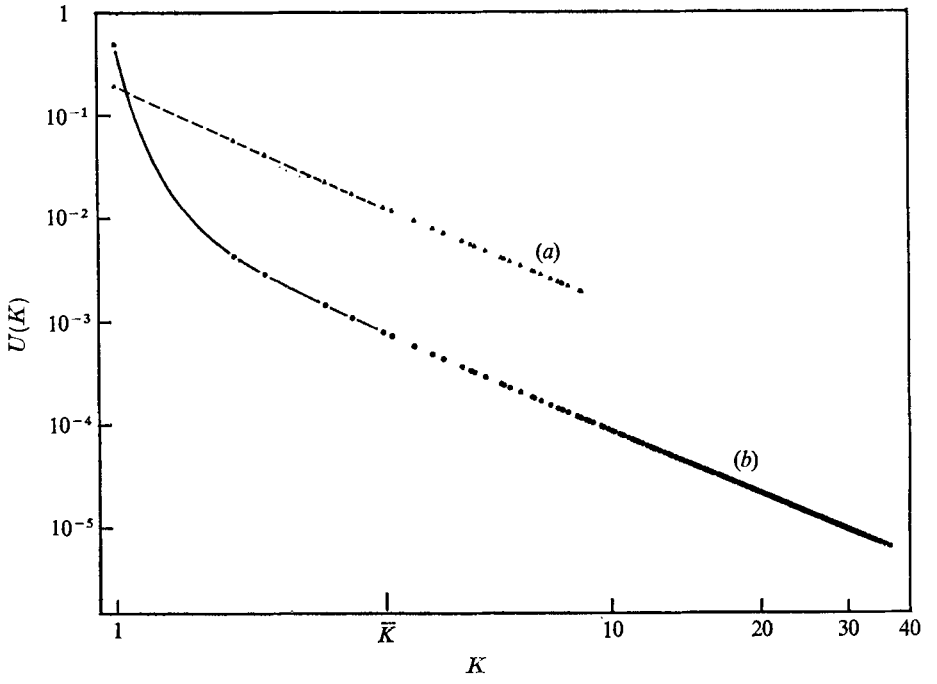

FIGURE 2. Theoretical spectra for $E = 3{\cdot}141$ and $\bar{K} = 3{\cdot}5$ (log–log scale). (*a*) 16×16 grid. (*b*) 64×64 grid.

when $k_n \to \infty$ as $n \to \infty$. That is, when we include higher and higher modes in the system, all the energy flows back into the lowest mode, with equipartition of enstrophy in the higher Fourier modes (figure 2). This peculiar behaviour may account for the insufficient magnitude of the eddy kinetic energy relative to the mean zonal kinetic energy in numerical models of the general circulation of the atmosphere (see for instance Somerville *et al.* 1973). It is thus a simple consequence of truncation itself that energy is not distributed in an inviscid numerical model as it is in real flows: an accurate statistical representation of subgrid scale motions is thus essential for recovering the real spectral properties of geophysical flows.

If, instead of adding higher modes to the system, we keep K_n fixed and make $n \to \infty$ by adding lower modes, so that $K_1 \to 0$, then the asymptotic energy spectrum has the following form:

$$\left.\begin{aligned} U(K_i) &= \frac{E}{N}\frac{K_n^2 - \bar{K}^2}{K_n^2 - K_i^2} \quad (i < n), \\ U(K_n) &= \frac{E}{\alpha_n}\frac{\bar{K}^2}{K_n^2}. \end{aligned}\right\} \tag{9}$$

That is, in that case all the enstrophy flows up into the highest mode, and there is equipartition of energy in the lower Fourier modes.

It should be kept in mind that $U(K_i)$ is the two-dimensional energy spectrum. The usual one-dimensional spectrum $E(K)$ is not well formulated in the case of

a discrete Fourier space. However, we may define an approximate spectrum $E(K)$ proportional to $KU(K)$. Expression (8) leads to an asymptotic form of $E(K)$ proportional to K^{-1} in the large wavenumber limit, while (9) yields a spectrum $E(K)$ proportional to K in the small wavenumber limit.

These approximate forms are consistent with the asymptotic equilibrium states

$$U(K) = a/(b + K^2) \tag{10}$$

obtained by Kraichnan (1967) from the viewpoint of macrocanonical ensemble averages. Indeed, Fox & Orszag (1973) showed that, energy and enstrophy being given, it is always possible to find unique real values of a and b such that (10) is a possible state of the system. Further, one can show that, when the number of degrees of freedom increases to infinity, b has the following limit:

$$\lim b = \begin{cases} -K_1^2 & \text{as} \quad K_n \to \infty \quad \text{with } K_1 \text{ fixed,} \\ -K_n^2 & \text{as} \quad K_1 \to 0 \quad \text{with } K_n \text{ fixed.} \end{cases}$$

However, figure 4 shows that this asymptotic form is not a good approximation of the spectrum in the case of low resolution.

5. Numerical experiments

The validity of the ergodic hypothesis can be tested by performing numerical integrations of the inviscid truncated equations: one can then verify whether the time averages of the spectral distribution of energy converge towards the theoretical values. The experiments were performed for the case of low-order systems, where the statistical equilibrium is reached after a reasonable amount of computing time. Moreover, the theoretical formulae were found to be accurate enough in the low-order case.

In all experiments, we used a truncated Jacobian J defined in finite-difference form on a regular triangular grid, conserving both energy and enstrophy (Sadourny, Arakawa & Mintz 1968). Rhombic periodicity was assumed along the directions of two unit vectors $\mathbf{e}_1$ and $\mathbf{e}_2$, with $(\mathbf{e}_1, \mathbf{e}_2) = \frac{2}{3}\pi$. In some experiments, the Laplacian was directly defined in spectral form, leading to pseudo-wavenumbers K defined by

$$K^2 = \tfrac{2}{3}[(\mathbf{k}\,.\,\mathbf{e}_1)^2 + (\mathbf{k}\,.\,\mathbf{e}_2)^2 + (\mathbf{k}\,.\,\mathbf{e}_3)^2] \quad (= |\mathbf{k}|^2),$$

with $\mathbf{e}_3 = -\mathbf{e}_1 - \mathbf{e}_2$. In other experiments, the seven-point finite-difference Laplacian was used instead, leading to a different definition of K:

$$K^2 = (8/3d^2)\,[\sin^2(\tfrac{1}{2}d\mathbf{k}\,.\,\mathbf{e}_1) + \sin^2(\tfrac{1}{2}d\mathbf{k}\,.\,\mathbf{e}_2) + \sin^2(\tfrac{1}{2}d\mathbf{k}\,.\,\mathbf{e}_3)]$$

(here d is the mesh distance). The isolines of K in the truncated Fourier space, giving the corresponding orders of multiplicity of the Fourier modes, are shown in figure 3.

In theory, the equilibrium spectrum is uniquely determined by the energy and enstrophy of the initial flow. This property was verified by performing separate experiments using widely different initial repartitions of energy: in some cases, the initial state was chosen in such a way that only three modes were excited,

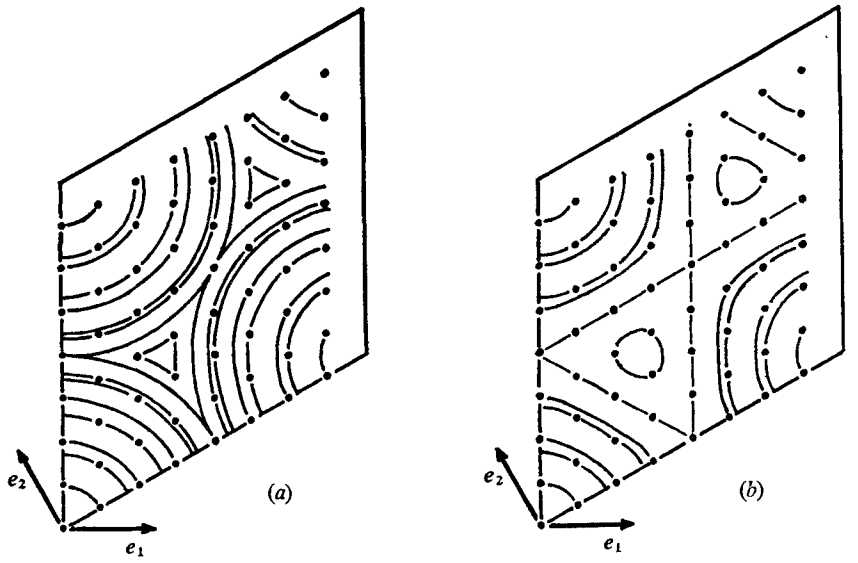

FIGURE 3. Isolines of K for an 8×8 grid. (*a*) For spectral truncation of the Laplacian. (*b*) With the simplest second-order finite-difference Laplacian.

corresponding to the vertices of two conjugate triangular meshes. This choice ensures that all Fourier modes are linear combinations of the initially excited modes and can therefore be excited in the further integration of the equations of motion, meaning that the trajectory in phase space is not singular, i.e. not contained in a submanifold of measure zero. In other cases, the full spectrum was excited initially using

$$\hat{\psi}(\mathbf{k}, 0) = R(\mathbf{k}) f(K) \tag{11}$$

by modulating a random excitation $R(\mathbf{k})$ by a prescribed function f of the pseudo-wavenumber. The time integration scheme was second-order centred (leapfrog) with a time average of odd and even solutions every 100 time steps. In all cases there was a slow dissipation of energy and enstrophy due to the time-averaging procedure. However, the relative damping was of the order of 10^{-8} per time step. For ergodic time scales of about 10^5 steps, this damping can be considered so slow that it does not perturb the ergodic properties.

The first experiment was designed to check the validity of the analytical formula (6) in the case of a system of very low order where asymptotic estimates such as (10) or (A 4) are far from accurate. The integration was performed on an 8×8 grid, using the finite-difference Laplacian. In that case, K varies from 0·883 to 2·426 (arbitrary units). The modes excited at $t = 0$ correspond to

$$K_3 = 1{\cdot}633, \quad K_4 = 2, \quad K_5 = 2{\cdot}134,$$

the average pseudo-wavenumber being $\overline{K} = 1{\cdot}88$. The time averages were computed over 40 000 time steps. Concurrently, a Monte Carlo method was used to compute the phase-space integrals involved in the calculation of the exact equilibrium spectrum (6). The two results are undistinguishable on figure 4, proving accurate convergence of the time averages to theoretical values. The

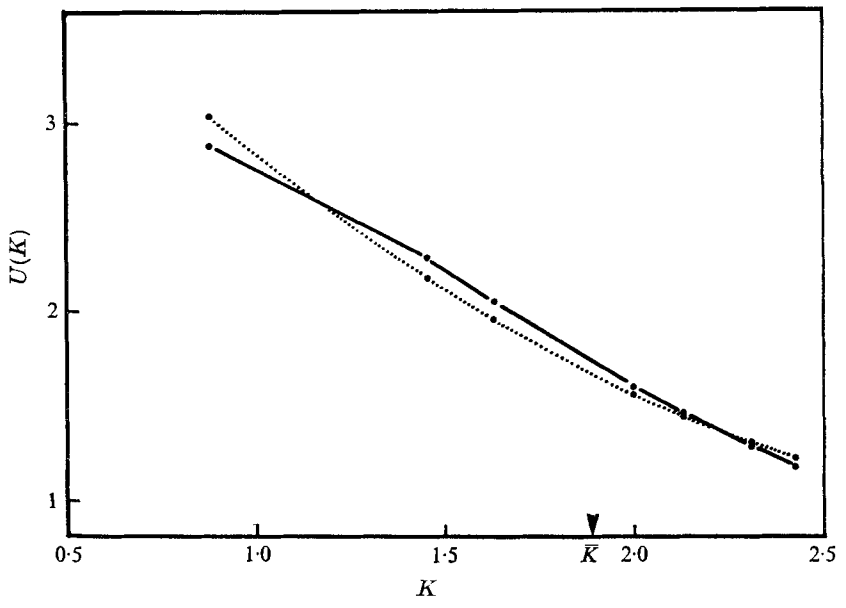

FIGURE 4. Verification of the ergodic hypothesis in the case of an 8×8 grid. ——, exact theoretical spectrum obtained from formula (6), as well as time-averaged spectrum of the numerical solution; ·····, approximate equilibrium spectrum obtained from Kraichnan's formula.

validity of the ergodic hypothesis in this particular case involving a low-order system is thus verified. The corresponding energy distribution of the form $U(\mathbf{k}) = a/(b+K^2)$ based on macrocanonical ensemble averages is significantly inaccurate in this case (figure 4).

The second and third experiments were performed on a 16×16 grid. The second experiment used a spectral Laplacian ($K = |\mathbf{k}|$). The wavenumbers extend from 1 to 8·71. At $t = 0$, the excited modes correspond to

$$K_3 = 2, \quad K_4 = 2{\cdot}64, \quad K_5 = 3,$$

the average wavenumber being $\bar{K} = 2{\cdot}43$. There is also very good agreement between the time averages and the expectations after the somewhat longer time of 98 000 steps (figure 5*a*). In this case, we are close to the asymptotic form, with almost all the energy in the first mode and equipartition of enstrophy in the higher modes.

The third experiment used the finite-difference Laplacian on the same grid. The pseudo-wavenumber varies from 1·147 to 6·218. The initially excited modes are at the higher end of the spectrum:

$$K_{23} = 6{\cdot}102 \quad \text{(two Fourier modes excited)},$$
$$K_{25} = 6{\cdot}218.$$

Figure 5 (*b*) shows the agreement between time averages and expectations after 95 000 steps. We are here closer to the second asymptotic form.

Finally, a series of experiments was performed using the 16×16 grid and

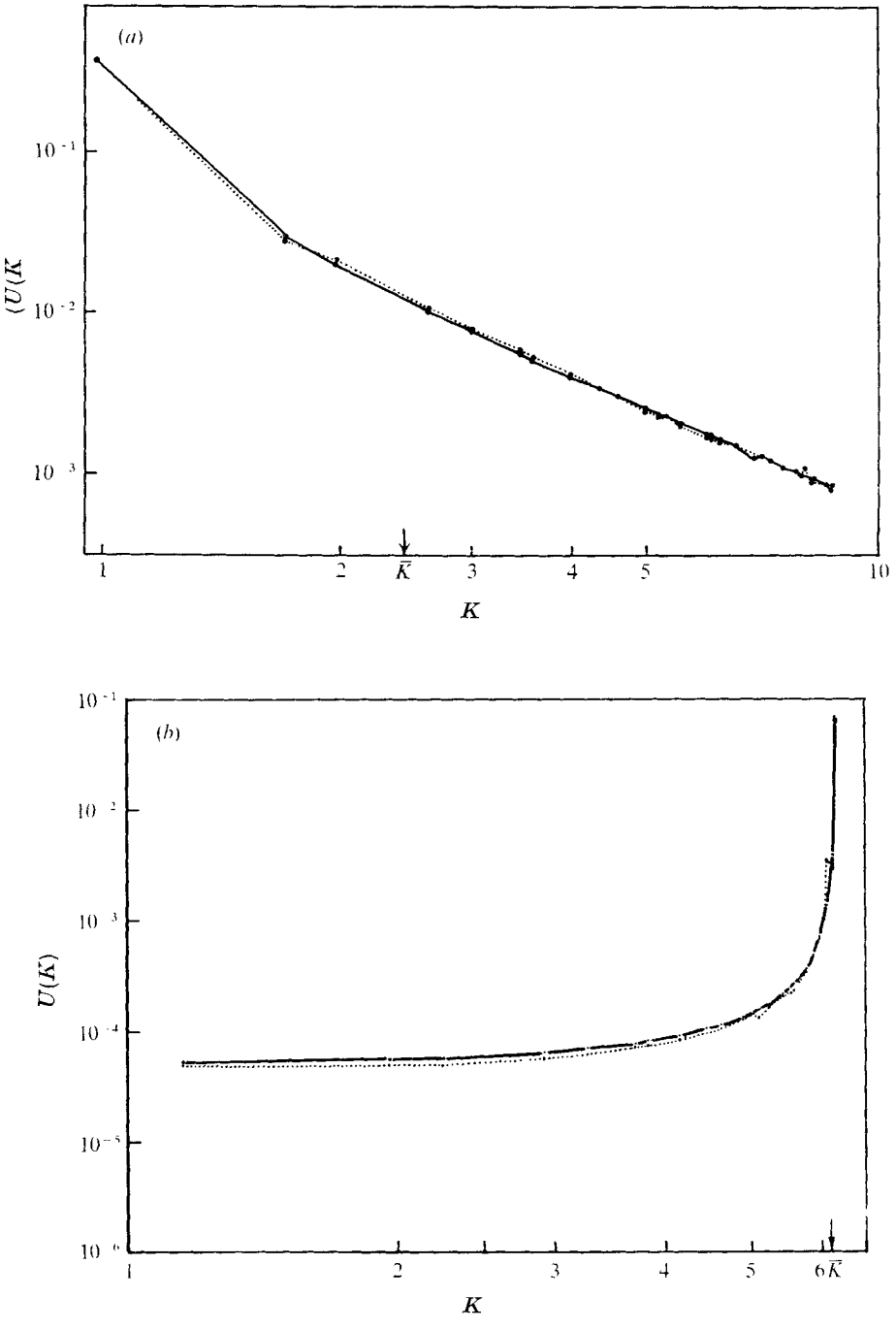

FIGURE 5. Verification of the convergence of the time-averaged spectrum to the theoretical spectrum for a 16×16 grid (log–log scale). (*a*) $\bar{K} = 2{\cdot}43$. (*b*) $\bar{K} = 6{\cdot}14$. ——, theoretical values; ·····, time averages after (*a*) 98 000 and (*b*) 95 000 steps.

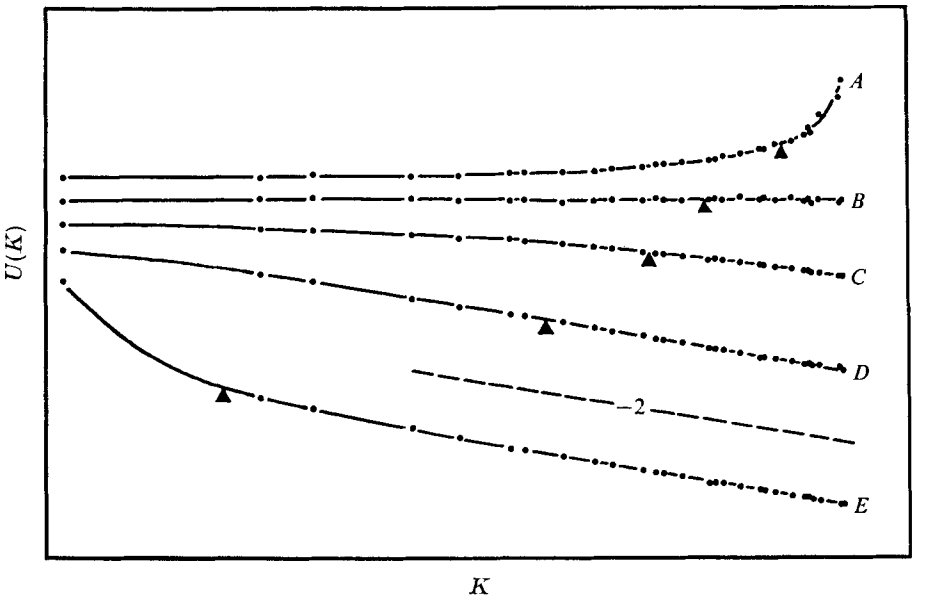

FIGURE 6. Various shapes of the equilibrium spectra (16 × 16 grid) obtained from numerical integrations after 40 000 steps (log–log scale). ▲, value of $\bar{K}$ corresponding to each spectrum. The scale is omitted; the slope −2, corresponding to equipartition of enstrophy, is indicated.

starting from fully excited spectra (11), with various forms of the modulating function $f(K)$ allowing widely different values of $\bar{K}$:

$$\begin{aligned}
&(A)\quad f(K) = K, && \bar{K} = 7{\cdot}34,\\
&(B)\quad f(K) = K^{-1}, && \bar{K} = 5{\cdot}95,\\
&(C)\quad f(K) = K^{-\frac{3}{2}}, && \bar{K} = 5{\cdot}08,\\
&(D)\quad f(K) = K^{-2}, && \bar{K} = 3{\cdot}81,\\
&(E)\quad f(K) = K^{-3}, && \bar{K} = 1{\cdot}57.
\end{aligned}$$

The corresponding time-averaged energy spectra are displayed in figure 6. Cases A and E produce equilibrium spectra similar to those already found in the third and second experiments (figures 5*b*, *a*) with similar orders of magnitude for $\bar{K}$. Cases B, C and D produce intermediate shapes. In case B, where we started from approximate equipartition of energy, the equilibrium spectrum remains close to exact equipartition. In case D, where enstrophy is roughly equally distributed among the Fourier modes at $t = 0$, the time averages show that equipartition of enstrophy is maintained. Case C is intermediate between energy equipartition and enstrophy equipartition; the time-averaged spectrum evolves towards an equilibrium shape where equipartition of energy approximately holds among the smaller wavenumbers, while approximate equipartition of enstrophy takes place among higher wavenumbers. In the case of a 16 × 16 grid, Kraichnan's formula is accurate enough to describe the equilibrium spectra: all time averages reproduced in figure 6 are indeed consistent with (10).

6. Conclusion

Assuming the 'mixing' hypothesis only, we have derived an exact analytical expression for the time-averaged energy spectrum of inviscid numerical models of two-dimensional incompressible flows. This expression is equally valid in the case of spectral models and finite-difference models constrained to exact energy and enstrophy conservation. Further, it is exact even in the case of a small number of degrees of freedom, where the asymptotic formula given by Kraichnan, based on macro-canonical ensemble averages, is far from accurate. Consequently it allows precise verification of the ergodic hypothesis even in the case of a low-order system. It turns out that Kraichnan's approximation is accurate for systems involving 16×16 points or more. A disadvantage of the present formulation is the absence of simple estimates in the general case. However, not only can such simple estimates be given in the particular cases where the mean pseudo-wavenumber is close to its minimum or maximum value, but upper and lower bounds can be derived in these cases: if the error in the estimates is known, convergence of the time averages of a numerical solution to the analytical expression can be accurately checked.

The ergodic hypothesis appears to be well verified in all cases investigated here. The theoretical spectra as well as the time averages are characterized by a tendency towards enstrophy equipartition at higher wavenumbers as long as the average wavenumber $\overline{K}$ is not too large. Conversely, a tendency towards energy equipartition is observed at smaller wavenumbers as long as $\overline{K}$ is not too small. There is thus a significant difference between the asymptotic behaviour of inviscid truncated systems and two-dimensional turbulence, characterized by the possibility of both an enstrophy cascade towards higher wavenumbers and a reverse energy cascade towards lower wavenumbers in the case of an infinite domain (e.g. Kraichnan 1967, 1971*b*; Lilly 1969; Frisch *et al.* 1974). By imposing zero transfer, truncations act as dams preventing possible cascades and imposing corresponding equipartitions 'upstream'. The key to more accurate statistical behaviour of numerical models is then a proper formulation of the enstrophy (or energy) transfer across the barriers imposed by the truncation. Some tentative solutions to this problem have already been proposed by Smagorinsky, Manabe & Holloway (1965) and Leith (1968, 1972) in the case of models of atmospheric flows.

Appendix A. Calculation of bounds for the theoretical spectrum

We shall consider only the somewhat restrictive case where β_2 is even, which is actually the case considered in our experimental computations, described in §5. The expression for U_i ($i \neq 2$) involves only integrals of the following type:

$$I = \int_V Y_2^{\beta_2} \prod_{j \neq 2} Y_j^{\gamma_j} dY_3 \dots dY_n. \tag{A 1}$$

We may consider V as the difference $V_2 - V_2'$, where V_2 is defined by (7) with

$Y_2 > 0$ and V_2' is defined by (7) with $Y_2 > 0$ and $Y_1 < 0$. The integration over V is now split into integrations over V_2 and V_2', which yields

$$I = I_2 - I_2'. \tag{A 2}$$

Instead of computing I_2', it is more convenient to calculate another integral I_1 over a volume V_1 defined by (7) with $Y_1 < 0$. Then our assumption on β_2 ensures that the integrand has the same sign throughout V_1. Hence

$$|I_2'| \leqslant |I_1|.$$

(Notice two simpler cases: if $K_1 \leqslant \bar{K} \leqslant K_2$ then $I_2' = 0$; if $K_2 \leqslant \bar{K} \leqslant K_3$ then $I_2' = I_1$.) This yields upper and lower bounds for I:

$$I_2 - |I_1| \leqslant I \leqslant I_2 + |I_1|. \tag{A 3}$$

It turns out that I_1 is in most cases extremely small compared with I_2, especially when the number of modes is large enough, so that we are able to compute I with very high accuracy.

In practice, we calculate only the integrals involved in U_i for $i > 2$, the remaining expectations U_1 and U_2 being obtained afterwards by making use of the two integral constraints. We define, for $i > 2$, $I(i)$, $I_1(i)$, $I_2(i)$ and $I_2'(i)$ as the integrals in which

$$\gamma_j = \beta_j, \quad j \neq 2, i,$$

$$\gamma_i = \beta_i + 1.$$

We also define $I(0)$, $I_1(0)$, $I_2(0)$ and $I_2'(0)$ as the same integrals with

$$\gamma_j = \beta_j, \quad j \neq 2.$$

Expressing (6), (A 1) and (A 2) in this notation, we get

$$U_i = \frac{1}{\alpha_i} \frac{I_2(i) - I_2'(i)}{I_2(0) - I_2'(0)},$$

or using (A 3), the approximate form

$$\frac{1}{\alpha_i} \frac{I_2(i) - |I_1(i)|}{I_2(0) + |I_1(0)|} \leqslant U_i \leqslant \frac{1}{\alpha_i} \frac{I_2(i) + |I_1(i)|}{I_2(0) - |I_1(0)|}. \tag{A 4}$$

We spare the reader rather cumbersome calculations and give at once the expressions for the various integrals which appear in (A 4) for the case $\beta_1 = \beta_2 = 2$, which was studied in our numerical experiments:

$$I_2(0) = A\left[d_0^2 - 2\frac{d_0 c_0}{S} R + \frac{c_0^2}{S(S+1)}(R^2 + F)\right],$$

$$I_1(0) = AD\left[c_0^2 - 2\frac{d_0 c_0}{S} T + \frac{d_0^2}{S(S+1)}(T^2 + G)\right]$$

and for $i > 2$

$$I_2(i) = A(\beta_i + 1)\frac{c_0}{c_i}\frac{E}{S}\left[d_0^2 - \frac{2d_0 c_0}{S+1}\left(R + \frac{d_i}{c_i}\right) + \frac{c_0^2}{(S+1)(S+2)}\left\{\left(R + \frac{d_i}{c_i}\right)^2 + F + \frac{d_i^2}{c_i^2}\right\}\right],$$

$$I_1(i) = A(\beta_i + 1)\frac{d_0}{d_i}\frac{E}{S} D\left[c_0^2 - \frac{2d_0 c_0}{S+1}\left(T + \frac{c_i}{d_i}\right) + \frac{d_0^2}{(S+1)(S+2)}\left\{\left(T + \frac{c_i}{d_i}\right)^2 + G + \frac{c_i^2}{d_i^2}\right\}\right],$$

with $c_i = K_i^2 - K_1^2$, $c_0 = \bar{K}^2 - K_1^2$, $d_i = K_i^2 - K_2^2$, $d_0 = \bar{K}^2 - K_2^2$,

$$S = \sum_{i=3}^{n} (\beta_i + 1) + 3, \quad R = \sum_{i=3}^{n} \frac{d_i}{c_i} (\beta_i + 1),$$

$$T = \sum_{i=3}^{n} \frac{c_i}{d_i} (\beta_i + 1), \quad F = \sum_{i=3}^{n} \frac{d_i^2}{c_i^2} (\beta_i + 1), \quad G = \sum_{i=3}^{n} \frac{c_i^2}{d_i^2} (\beta_i + 1),$$

$$A = c_2^{-4} E^{S+1} \frac{\Gamma(3)}{\Gamma(S)} \left(\prod_{i=3}^{n} \Gamma(\beta_i + 1) \right) c_0^2 \left\{ \prod_{i=3}^{n} \left(\frac{c_0}{c_i} \right)^{\beta_i + 1} \right\},$$

$$D = \frac{d_0^2}{c_0^2} \prod_{i=3}^{n} \left(\frac{d_0}{c_0} \frac{c_i}{d_i} \right)^{\beta_i + 1}.$$

Appendix B. Asymptotic behaviour of the expected spectra

We shall first be interested in the asymptotic behaviour of the spectrum when K_1 is fixed and $K_n \to \infty$ as $n \to \infty$. In this case, $S \to \infty$ and $d_n/c_n \to 1$, so that R, T, F and G are equivalent to S. Further, if $\bar{K} > K_2$

$$S^{-1} \log D \to \log (d_0/c_0) < 0,$$

so that $D \to 0$ exponentially. (If $\bar{K} \leqslant K_2$, $I_2' = 0$.) We then have

$$A^{-1} I_2(0) \sim (d_0 - c_0)^2, \quad A^{-1} I_1(0) \sim D (d_0 - c_0)^2,$$

$$A^{-1} I_2(i) \sim (\beta_i + 1) \frac{c_0}{c_i} \frac{E}{S} (d_0 - c_0)^2,$$

$$A^{-1} I_1(i) \sim (\beta_i + 1) \frac{d_0}{d_i} \frac{E}{S} D (d_0 - c_0)^2,$$

so that

$$U_i \sim \frac{c_0}{c_i} \frac{E}{2S} \sim \frac{E}{N} \frac{\bar{K}^2 - K_1^2}{K_i^2 - K_1^2} \quad (i > 2).$$

We need now to study the asymptotic behaviour of U_1 and U_2. From the constraints on energy and enstrophy, we get

$$\alpha_2 c_2 U_2 = c_0 E - \sum_{i=3}^{n} \alpha_i c_i U_i,$$

or using the notation of appendix A,

$$\alpha_2 c_2 U_2 = \left\{ \left(c_0 E A^{-1} I_2(0) - \sum_{i=3}^{n} c_i A^{-1} I_2(i) \right) - \left(c_0 E A^{-1} I_2'(0) - \sum_{i=3}^{n} c_i A^{-1} I_2'(i) \right) \right\} \Big/ A^{-1} I(0).$$

From the inequalities derived in appendix A, we thus get

$$\left| c_0 E A^{-1} I_2'(0) - \sum_{i=3}^{n} c_i A^{-1} I_2'(i) \right| \leqslant c_0 E A^{-1} I_1(0) + \sum_{i=3}^{n} c_i A^{-1} I_1(i),$$

and using the analytic form of I_1, we write

$$\sum_{i=3}^{n} c_i A^{-1} I_1(i) = D d_0 \frac{E}{S} \left[c_0^2 T - \frac{2 d_0 c_0}{S+1} (T^2 + G) + \frac{d_0^2}{(S+1)(S+2)} \left(T^3 + 3TG + 2 \sum_{i=3}^{n} \frac{c_i^3}{d_i^3} (\beta_i + 1) \right) \right].$$

The right-hand side is obviously equivalent to D. Further,

$$c_0 EA^{-1}I_2(0) - \sum_{i=3}^{n} c_i A^{-1}I_2(i) = \frac{3}{S} c_0 E\left[d_0^2 - \frac{2d_0c_0R}{S+1} + \frac{c_0^2}{S+1}\frac{R^2+F}{S+2}\right]$$

$$\sim \frac{3}{S} c_0 E(d_0 - c_0)^2,$$

and using the asymptotic behaviour of $A^{-1}I_2(0)$ and $A^{-1}I_1(0)$, we get

$$U_2 \sim \frac{1}{\alpha_2}\frac{3}{S}\frac{c_0}{c_2} E \sim \frac{E}{N}\frac{\bar{K}^2 - K_1^2}{K_2^2 - K_1^2}.$$

We now calculate U_1. Again, from the constraints on energy and enstrophy,

$$\alpha_1 c_2 U_1 = \sum_{i=3}^{n} d_i \alpha_i U_i - d_0 E.$$

So with the notation of appendix A,

$$\alpha_1 c_2 U_1 = \left(\sum_{i=3}^{n} d_i A^{-1}I_2(i) - d_0 EA^{-1}I_2(0)\right)\Big/ A^{-1}I(0)$$

$$- \left(\sum_{i=3}^{n} d_i A^{-1}I_2'(i) - d_0 EA^{-1}I_2'(0)\right)\Big/ A^{-1}I(0).$$

As in the case of U_2, we get a bound for the numerator of the second term:

$$\left|\sum_{i=3}^{n} d_i A^{-1}I_2'(i) - d_0 EA^{-1}I_2'(0)\right| \leqslant \sum_{i=3}^{n} d_i A^{-1}I_1(i) + d_0 EA^{-1}I_1(0),$$

and evaluating the sum on the right-hand side gives

$$\sum_{i=3}^{n} d_i A^{-1}I_1(i) = Dd_0 \frac{E}{S}\left[c_0^2(S-3) - \frac{2d_0c_0}{S+1} T(S-2)\right.$$

$$\left. + \frac{d_0^2}{(S+1)(S+2)} (T^2+G)(S+1)\right].$$

We see that this term is of the same order of magnitude as D. On the other hand, we have

$$\sum_{i=3}^{n} d_i A^{-1}I_2(i) - d_0 EA^{-1}I_2(0) = E\left[d_0^2\left(c_0\frac{R}{S} - d_0\right)\right.$$

$$- \frac{2d_0c_0}{S}\left(c_0\frac{R^2+F}{S+1} - d_0R\right) + \frac{c_0^2}{S(S+1)}\left\{\frac{c_0}{S+2}\left(R^3 + 3RF\right.\right.$$

$$\left.\left. + 2\sum_{i=3}^{n}\frac{d_i^3}{c_i^3}(\beta_i+1)\right) - d_0(R^2+F)\right\}\Big] \sim E(c_0-d_0)(d_0-c_0)^2.$$

Hence using the asymptotic behaviour of $I(0)$,

$$U_1 \sim \frac{1}{\alpha_1}\frac{(c_0-d_0)E}{c_2} = \frac{E}{\alpha_1}.$$

Lastly, we are interested in the asymptotic behaviour of the spectrum when K_n is fixed and $K_1 \to 0$ as $n \to \infty$. This will be obtained in the simplest way by

interchanging energy and enstrophy and considering K_i^{-1} instead of K_i in the preceding calculations. Thus, the asymptotic spectrum is in this case

$$U_i = \frac{E}{N}\frac{K_n^2 - \bar{K}^2}{K_n^2 - K_i^2} \quad (i < n), \quad U_n = \frac{E}{\alpha_n}\frac{\bar{K}^2}{K_n^2}.$$

REFERENCES

Arakawa, A. 1966 Computational design for long-term numerical integration of the equations of fluid motion: two-dimensional incompressible flow (part 1). *J. Comp. Phys.* **1**, 119–143.

Deem, G. S. & Zabusky, N. J. 1971 Ergodic boundary in numerical simulations of two-dimensional turbulence. *Phys. Rev. Lett.* **27**, 396–399.

Fox, D. G. & Orszag, S. A. 1973 Inviscid dynamics of two-dimensional turbulence. *Phys. Fluids*, **16**, 167–171.

Frisch, U., Lesieur, M. & Brissaud, A. 1974 A Markovian random coupling model for turbulence. *J. Fluid Mech.* **65**, 145–152.

Khinchin, A. I. 1949 *Mathematical Foundations of Statistical Mechanics.* Dover.

Kraichnan, R. H. 1967 Inertial ranges in two-dimensional turbulence. *Phys. Fluids*, **10**, 1417–1423.

Kraichnan, R. H. 1971*a* An almost-Markovian Galilean-invariant turbulent model. *J. Fluid Mech.* **47**, 513–524.

Kraichnan, R. H. 1971*b* Inertial-range transfer in two- and three-dimensional turbulence. *J. Fluid Mech.* **47**, 525–535.

Leith, C. E. 1968 Two-dimensional eddy viscosity coefficients. *Proc. W.M.O./I.U.G.G. Symp. Numer. Weather Prediction, Tokyo*, vol. 1, pp. 41–44.

Leith, C. E. 1972 *Internal Turbulence. Conf. on Parametrization of Sub-grid Scale Processes, Leningrad.*

Lilly, D. K. 1969 Numerical simulation of two-dimensional turbulence. *Phys. Fluids Suppl.* **12**, II 240.

Onsager, L. 1949 Statistical hydrodynamics. *Nuovo Cimento Suppl.* **6**, 279–286.

Orszag, S. A. 1970 Analytical theories of turbulence. *J. Fluid Mech.* **41**, 363–386.

Sadourny, R., Arakawa, A. & Mintz, Y. 1968 Integration of the non divergent barotropic vorticity equation with an icosahedral–hexagonal grid for the sphere. *Mon. Weather Rev.* **96**, 351–356.

Smagorinsky, J., Manabe, S. & Holloway, J. L. 1965 Numerical results from a nine-level general circulation model of the atmosphere. *Mon. Weather Rev.* **93**, 727–768.

Somerville, R. C. J., Stone, P. M., Halem, M., Hansen, J. E., Hogan, J. S., Druyan, L. M., Russell, G., Lacis, A. A., Quirk, W. J. & Tenenbaum, J. 1973 The GISS Model of the global atmosphere. *Rep. Inst. Space Studies, Goddard Space Flight Center, N.A.S.A., New York.*